

SWITCHING ACTIVITY IN AN ENSEMBLE OF EXCITABLE NEURONS

A. G. Korotkov¹, S. Y. Zagrebin¹, and G. V. Osipov¹

¹Department of Control Theory and System Dynamics, Scientific and Educational Mathematical Center “Mathematics of future technologies”

Abstract

The paper proposes two dynamical systems based on the generalized Lotka-Volterra model of three excitable elements interacting through excitatory couplings. It is shown that for some values of the coupling parameters in the phase space of systems, there are heteroclinic cycles containing three or six saddle equilibrium states and heteroclinic curves connecting them. Under certain external stimuli that transfer the system from a stable zero equilibrium state to a small neighborhood of the heteroclinic cycle, the phase trajectory will alternately visit the neighborhood of saddle equilibrium states (possibly more than once), after which it will return to its initial state. The described behavior is proposed to be used to simulate switching activity in neural ensembles. Different transients are determined by different external stimuli. The passage of the phase point of the system near the saddle equilibrium states included in the heteroclinic circuit is proposed to be interpreted as activation of the corresponding element.

1 Introduction

Often, dynamic processes in neural ensembles are sequential switches of activity between individual neurons and/or groups of neurons. This type of activity is associated with many physiological functions of the nervous system. The generation and propagation of excitation sequences between neurons or groups of them play a crucial role in the brain functioning. For example, sequential activity is observed in neural networks of sensory and motor systems of animals [1]. In addition, the regions of the brain responsible for the reproduction of singing in the brain of birds is the one that generates sequences of bursting activity [2]. A number of examples where excitation sequences play a key role can be continued [3,4].

Currently, an urgent task is to study sequential neural activity through the theory of dynamical systems. In [1] it was hypothesized that sequential activity may be a consequence of the presence of a stable heteroclinic contour in the phase space of a dynamic system modeling the dynamics of a neural network [5–8]. According to it, the basis of the transient dynamics is the winnerless competition principle [9–11]. In short, the essence of this principle is the existence of a stable heteroclinic contour between trajectories of saddle type (these can be saddle equilibrium states, saddle limit cycles, etc.) [12–15]. When the representative point is in a small neighborhood of the saddle trajectory, it is assumed that a certain element of the network (neuron or group of neurons) corresponding to this saddle trajectory is activated. Thus, a stable heteroclinic contour in phase space is a mathematical image of sequential switching of activity in neural motifs. It was shown in [12] that such a contour exists in ensembles with inhibitory couplings.

Traditionally, in dynamical systems, the main attention is paid to asymptotic modes (at $t \rightarrow \infty$), and transition processes are discarded. However, in neural motifs, the transition process is often more important than the attractor [16–18]. This fact brings some specifics to the study of models of neural ensembles: for example, it may matter whether it is a stable equilibrium state, a node or a focus (this

difference is usually neglected when studying only the asymptotic properties of a dynamical system). The presence/absence of saddle limit cycles, etc., may also be important.

The main attention in the work will be paid to the study of transition processes associated with the presence of heteroclinic contours: closed contours consisting of one-dimensional heteroclinic trajectories connecting saddle special trajectories. In the models under consideration, these are saddle equilibrium states.

Mathematical models of neural ensembles can be divided into two types: microscopic level models (cell level) and large-scale models (neural ensembles level). In the first type models each neuron of an ensemble is modeled by a system of differential or difference equations, and connections are established between neurons (which can also be modeled by a system of differential or difference equations).

The second type includes Wilson-Cowan models and generalized Lotka-Volterra models. These models describe the interaction between populations of neurons. In this paper, a generalized Lotka-Volterra model is used to model a neural motif.

2 The first type system

In this section we will study the dynamics of the activity of neural ensembles consisting of elements modeled by the following equation

$$\dot{\rho} = \rho(\rho - 1). \quad (1)$$

Here and further, the variable ρ describes the activity of a neuron. The neuron is inactive when $\rho = 0$ and active when $\rho > 0$. The maximum activity takes place at $\rho = 1$. The paper assumes to consider the interval of change of ρ from 0 to 1. The dynamics of the system described by the Eq. (1) is trivial. The equilibrium state $\rho_1 = 0$ is stable. The equilibrium state $\rho_2 = 1$ is unstable. At $\rho = 0$, the individual neuron is in an unexcited (inactive) state. In the study of the dynamics of neural ensembles, it will be assumed that all the neurons of the ensemble are not excited at the initial moment of time. The excitation of neurons will occur due to the supply of external stimuli.

We will analyze the dynamics of the ensemble of their three elements. The dynamical system in this case is a special case of the generalized Lotka-Volterra model and has the form

$$\begin{cases} \dot{\rho}_1 = \rho_1(\rho_1 - 1 + \alpha\rho_2 + \beta\rho_3) + a\delta(\rho_1) \\ \dot{\rho}_2 = \rho_2(\rho_2 - 1 + \alpha\rho_3 + \beta\rho_1) + b\delta(\rho_2) \\ \dot{\rho}_3 = \rho_3(\rho_3 - 1 + \alpha\rho_1 + \beta\rho_2) + c\delta(\rho_3) \end{cases}, \quad (2)$$

where $\delta(x)$ is Dirac delta function. a, b, c , parameters are amplitudes of the external stimulus on each element. α and β parameters define the couplings between the elements. The paper will consider only the case of $\alpha > 0$, $\beta > 0$, which corresponds to the case of excitatory couplings.

2.1 A study of a two-dimensional system on an invariant plane $\rho_3 = 0$

Since one of the conditions $\rho_i = 0$ is met, the i -th equation of Eqs. (2) turns into an identity, then the three planes $\rho_i = 0$ are invariant. To understand the dynamics in a three-dimensional space, we first consider the behavior of two-dimensional systems on the invariant planes $\rho_i = 0$.

On the invariant plane $\rho_3 = 0$ Eqs. (2) takes the form

$$\begin{cases} \dot{\rho}_1 = \rho_1(\rho_1 - 1 + \alpha\rho_2) \\ \dot{\rho}_2 = \rho_2(\rho_2 - 1 + \beta\rho_1) \end{cases}. \quad (3)$$

This system describes the interaction of two interconnected elements.

The equilibrium states of Eqs. (3) and their eigenvalues are given in Table 1.

Equilibrium state	Eigenvalues	
$O_1(0, 0)$	-1	-1
$O_2(1, 0)$	1	$\beta - 1$
$O_3(0, 1)$	1	$\alpha - 1$
$O_4(\frac{\alpha-1}{\alpha\beta-1}, \frac{\beta-1}{\alpha\beta-1})$	1	$\frac{(1-\alpha)(\beta-1)}{\alpha\beta-1}$

Table 1: Steady states of Eqs. (3) and it's eigenvalues.

Let us define the types of equilibrium states of Eqs. (3) depending on the values of the α and β parameters.

1. O_1 is always a stable node;
2. In the region A ($0 < \alpha, \beta < 1$), the equilibria O_2 and O_3 are saddles, O_4 is an unstable node.
3. In the region B ($0 < \beta < 1 < \alpha$), O_2 is a saddle, O_3 is an unstable node, O_4 has one negative coordinate (at $\alpha\beta \neq 1$).
4. In the region C ($0 < \alpha < 1 < \beta$), O_2 is an unstable node, O_3 is a saddle, O_4 has one negative coordinate (at $\alpha\beta \neq 1$).
5. In the region D ($\alpha, \beta > 1$), the equilibria O_2 and O_3 are unstable nodes, O_4 is a saddle.

Since the negative values of ρ_i are not considered, there are three equilibrium states in the regions B and C, and they lie on the ρ_1 and ρ_2 axes.

Figure 1 shows the partitioning of the parameter plane into the regions A, B, C, D and the corresponding phase portraits.

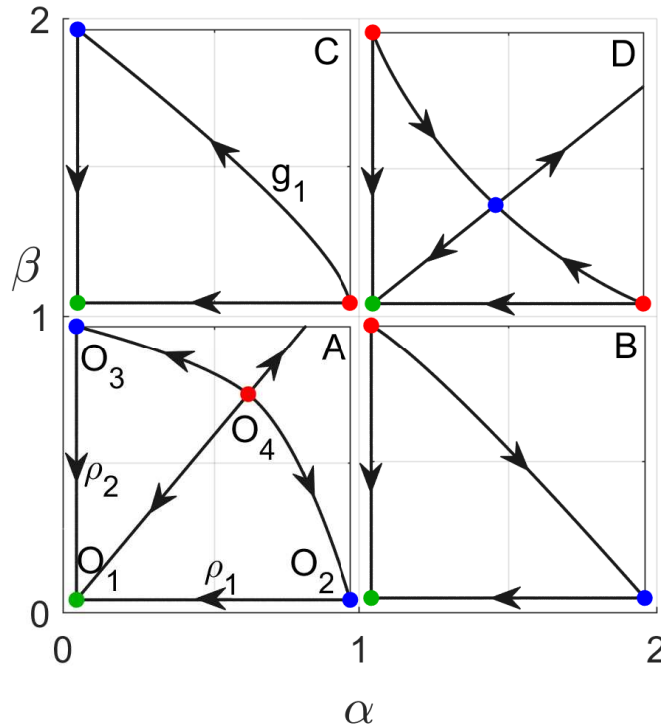


Figure 1: Different types of phase portraits of Eqs. (3).

In all subsequent figures the following notation is used: blue dots correspond to saddle equilibrium states, green - to stable, red - to unstable.

Using the Bendixon-Dulac theorem, we show that there are no limit cycles in the phase space of the model (3) in the region $\rho_{1,2} > 0$. Indeed,

$$\frac{\partial}{\partial \rho_1} \frac{\dot{\rho}_1}{\rho_1 \rho_2} + \frac{\partial}{\partial \rho_2} \frac{\dot{\rho}_2}{\rho_1 \rho_2} = \frac{\partial}{\partial \rho_1} \frac{\rho_1 - 1 + \alpha \rho_2}{\rho_2} + \frac{\partial}{\partial \rho_2} \frac{\rho_2 - 1 + \beta \rho_1}{\rho_1} = \frac{1}{\rho_2} + \frac{1}{\rho_1}.$$

Thus, $\frac{\partial}{\partial \rho_1} \frac{\dot{\rho}_1}{\rho_1 \rho_2} + \frac{\partial}{\partial \rho_2} \frac{\dot{\rho}_2}{\rho_1 \rho_2} > 0$ in the region $\rho_{1,2} > 0$, this means that there are no limit cycles in this region.

Let us consider the parameter region C (similarly, the region B is considered). On the plane (ρ_1, ρ_2) there is a trajectory g_1 going from the unstable node O_2 to the saddle O_3 . For the three-dimensional system considered below, this trajectory g_1 is heteroclinic, since in a three-dimensional system the equilibrium state O_3 is a saddle. Similarly, it is possible to show the presence of heteroclinic trajectories on the invariant planes $\rho_1 = 0$ and $\rho_2 = 0$. The heteroclinic cycle in a three-dimensional system consists precisely of such heteroclinic trajectories.

The system described by Eqs. (3) has one drawback. For the initial conditions lying below the curve g_1 , all trajectories come to a stable node O_1 . And for the initial conditions lying above the curve g_1 , all trajectories go to infinity. This disadvantage disappears in the second model, discussed below.

2.1.1 Bifurcations in a two-dimensional system

The analysis of the eigenvalues of the equilibria given in Table 1 allows us to determine the bifurcations occurring in Eqs. (3). At $\beta = 1$, the equilibrium states O_2 and O_4 undergo transcritical bifurcation. At $\alpha = 1$, the equilibrium states O_3 and O_4 also undergo transcritical bifurcation. At $\alpha\beta = 1$, the equilibrium state O_4 does not exist; when passing through this curve, the sign of one of the coordinates changes to the opposite. The bifurcation diagram of Eqs. (3) is shown in Fig. 1.

2.2 Dynamics of a three-neuron ensemble (Eqs. (2))

Eqs. (2) can have 8 equilibrium states. The coordinates of the equilibrium states and their eigenvalues are given in Table 2.

Equilibrium state	Eigenvalues		
$O_1(0, 0, 0)$	-1	-1	-1
$O_2(1, 0, 0)$	1	$\alpha - 1$	$\beta - 1$
$O_3(0, 1, 0)$	1	$\alpha - 1$	$\beta - 1$
$O_4(0, 0, 1)$	1	$\alpha - 1$	$\beta - 1$
$O_5(0, \frac{\alpha-1}{\alpha\beta-1}, \frac{\beta-1}{\alpha\beta-1})$	1	$\frac{\alpha^2+\beta^2-\alpha\beta-\alpha-\beta+1}{\alpha\beta-1}$	$\frac{(\alpha-1)(1-\beta)}{\alpha\beta-1}$
$O_6(\frac{\beta-1}{\alpha\beta-1}, 0, \frac{\alpha-1}{\alpha\beta-1})$	1	$\frac{\alpha^2+\beta^2-\alpha\beta-\alpha-\beta+1}{\alpha\beta-1}$	$\frac{(\alpha-1)(1-\beta)}{\alpha\beta-1}$
$O_7(\frac{\alpha-1}{\alpha\beta-1}, \frac{\beta-1}{\alpha\beta-1}, 0)$	1	$\frac{\alpha^2+\beta^2-\alpha\beta-\alpha-\beta+1}{\alpha\beta-1}$	$\frac{(\alpha-1)(1-\beta)}{\alpha\beta-1}$
$O_8(\frac{1}{\alpha+\beta+1}, \frac{1}{\alpha+\beta+1}, \frac{1}{\alpha+\beta+1})$	1	$\frac{2-\alpha-\beta+(\alpha-\beta)\sqrt{3}i}{2(\alpha+\beta+1)}$	$\frac{2-\alpha-\beta-(\alpha-\beta)\sqrt{3}i}{2(\alpha+\beta+1)}$

Table 2: The equilibrium states of Eqs. (2) and their eigenvalues.

Figure 2 shows the bifurcation diagram of Eqs. (2). The following are descriptions of equilibrium states in all regions of the diagram 2.

1. O_1 is a stable node.
2. In the region A ($0 < \alpha, \beta < 1$) the equilibria O_2, O_3 and O_4 are saddles with a two-dimensional stable manifold and a one-dimensional unstable manifold, the equilibria O_5, O_6 and O_7 are saddles with a one-dimensional stable manifold and a two-dimensional unstable manifold, the equilibrium state O_8 is an unstable focus (at $2 - \alpha - \beta < 1$) or a node.

3. In the regions B_1 ($\alpha > 1, \alpha + \beta < 2$) and C_1 ($\beta > 1, \alpha + \beta < 2$) the equilibria O_2, O_3 and O_4 are saddles with a two-dimensional unstable manifold and a one-dimensional stable manifold, the equilibria O_5, O_6 and O_7 are saddles with a one-dimensional unstable manifold and a two-dimensional stable manifold, the equilibrium state O_8 is an unstable focus.
4. In the regions B_2 ($\alpha > 1, \alpha + \beta > 2, \alpha\beta < 1$) and C_2 ($\beta > 1, \alpha + \beta > 2, \alpha\beta < 1$) the equilibria O_2, O_3 and O_4 are saddles with a two-dimensional unstable manifold and a one-dimensional stable manifold, the equilibria O_5, O_6 and O_7 are saddles with a one-dimensional unstable manifold and a two-dimensional stable manifold, the equilibrium state O_8 is a saddle-focus.
5. In the regions B_3 ($\beta < 1, \alpha\beta > 1$) and C_3 ($\alpha < 1, \alpha\beta > 1$) the equilibria O_2, O_3 and O_4 are saddles with a two-dimensional unstable manifold and a one-dimensional stable manifold, the equilibria O_5, O_6 and O_7 are unstable nodes, the equilibrium state O_8 is a saddle-focus.
6. In the region D ($\alpha, \beta > 1$) the equilibria O_2, O_3 and O_4 are unstable nodes, the equilibria O_5, O_6 and O_7 are saddles with a one-dimensional stable manifold and a two-dimensional unstable manifold, the equilibrium state O_8 is a saddle-focus.

When $\alpha\beta = 1$, the equilibria O_5, O_6, O_7 do not exist. In addition, at $\alpha + \beta = 2$ the real part of the two eigenvalues of the equilibrium state O_8 turns into 0. At $\alpha + \beta < 2$, this equilibrium state is an unstable saddle-focus with three unstable manifolds, at $\alpha + \beta > 2$, it is a saddle-focus with one-dimensional unstable and two-dimensional stable manifolds. Let's examine this bifurcation in detail.

When the condition is met $\alpha + \beta = 2$ we have

$$\begin{aligned} \dot{\rho}_1 + \dot{\rho}_2 + \dot{\rho}_3 &= \rho_1(\rho_1 - 1 + \alpha\rho_2 + (2 - \alpha)\rho_3) + \rho_2(\rho_2 - 1 + \alpha\rho_3 + (2 - \alpha)\rho_1) + \rho_3(\rho_3 - 1 + \alpha\rho_1 + (2 - \alpha)\rho_2) = \\ &= \rho_1^2 + \rho_2^2 + \rho_3^2 - \rho_1 - \rho_2 - \rho_3 + 2(\rho_1\rho_3 + \rho_2\rho_1 + \rho_3\rho_2) = (\rho_1 + \rho_2 + \rho_3)^2 - \rho_1 - \rho_2 - \rho_3. \end{aligned}$$

If $\rho_1 + \rho_2 + \rho_3 = 1$, we get the identity $0 = 0$. Therefore, the plane $\rho_1 + \rho_2 + \rho_3 = 1$ is an invariant set.

On the invariant plane $\rho_1 + \rho_2 + \rho_3 = 1$, provided $\alpha + \beta = 2$, Eqs. (2) takes the form

$$\begin{cases} \dot{\rho}_1 = (\alpha - 1)\rho_1(\rho_1 - 1 + 2\rho_2) \\ \dot{\rho}_2 = (1 - \alpha)\rho_2(\rho_2 - 1 + 2\rho_1) \end{cases} \quad (4)$$

This system can be transformed by substitution of time into

$$\begin{cases} \dot{\rho}_1 = -\rho_1(\rho_1 - 1 + 2\rho_2) \\ \dot{\rho}_2 = \rho_2(\rho_2 - 1 + 2\rho_1) \end{cases} \quad (5)$$

The solution of this system is

$$2\rho_1\rho_2^2 - 2\rho_1\rho_2(1 - \rho_1) - C = 0.$$

The diagrams of this function inside the region $\rho_{1,2} > 0, \rho_1 + \rho_2 < 1$ are closed curves. Thus, under the condition of $\alpha + \beta = 2$ on the invariant plane $\rho_1 + \rho_2 + \rho_3 = 1$ through each point of the set $\rho_{1,2,3} > 0$ a closed curve passes.

Figure 3 shows all the different types of phase portraits of Eqs. (2) for parameters from the regions shown in Fig. 2.

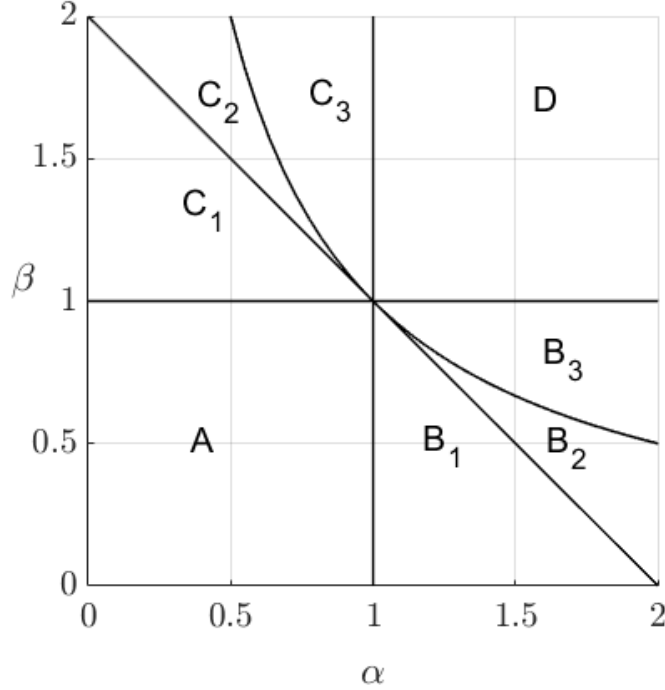


Figure 2: Bifurcation diagram of Eqs. (2).

The dynamics of an ensemble of three neurons, depending on the parameters, can be as follows:

1. For all regions (Fig. 3), depending on the external stimulus, the phase trajectories either come to a stable equilibrium state O_1 or go to infinity.
2. For the regions C_1 , C_2 and C_3 , the boundary between the basins of attraction of the equilibrium and infinity is the integral manifold M containing the saddle points O_2 , O_3 and O_4 and the saddle-focus O_8 .

In the previous section, it was shown that in the regions C_1 , C_2 and C_3 in the non-negative quadrant of the invariant plane $\rho_3 = 0$ there are three equilibrium states: a stable node $O_1(0,0)$, an unstable node $O_3(0,1)$ and a saddle $O_2(1,0)$. When adding the third coordinate ρ_3 , the equilibrium state $O_1(0,0,0)$ is a stable node, the equilibrium states $O_3(0,1,0)$ and $O_2(1,0,0)$ are saddles with a two-dimensional unstable manifold and a one-dimensional stable manifold. Between the saddle equilibrium states $O_2(1,0,0)$ and $O_3(0,1,0)$ there is a heteroclinic trajectory g_1 . Due to the symmetry of Eqs. (2), between pairs of saddles $O_3(0,1,0)$, $O_4(0,0,1)$ and $O_4(0,0,1)$, $O_2(1,0,0)$ there are also heteroclinic trajectories g_2 and g_3 , respectively. Thus, in the phase space of Eqs. (2) there is a heteroclinic cycle G connecting the saddles O_2 , O_3 and O_4 . Like the usual limit cycle, the heteroclinic cycle can be stable, unstable and saddle. This is determined by the stability (instability) of the manifolds forming this cycle at the intersection. The heteroclinic cycle G unstable at $\alpha + \beta < 2$ (manifolds ρ_1 , ρ_2 , ρ_3 and M are unstable) and saddle at $\alpha + \beta > 2$ (the manifold M is stable).

2.2.1 Sequential activity

As mentioned above, one of the behaviors of a neural ensemble is the alternate activation of neurons as a result of a response to an external stimulus, followed by the return of all neurons to their original non-excited state. Mathematical images of such behavior can be phase trajectories passing near the heteroclinic cycle G . In the model under consideration, this cycle is a closed trajectory consisting of heteroclinic curves connecting the saddle equilibrium states O_2 , O_3 , O_4 , i.e. the saddles lying on the axes. Only in the regions B_i and C_i these saddles have one-dimensional unstable manifolds that connect them. Thus, the sequential

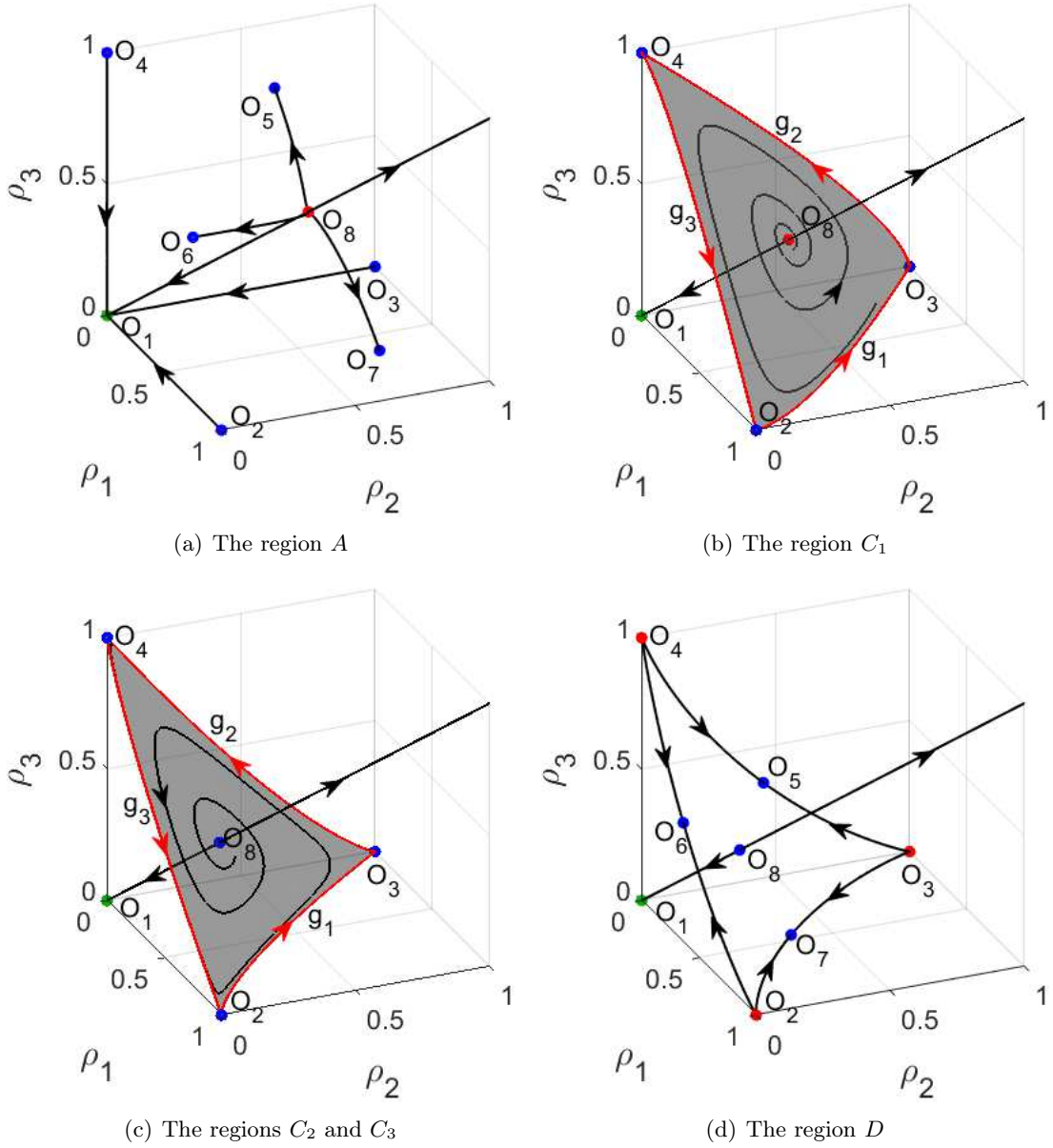


Figure 3: Various types of phase portraits of Eqs. (2). The heteroclinic trajectories forming the heteroclinic cycle G are shown in red in Figs. b) and c) the invariant manifold M is highlighted in gray. In the region C_1 , the manifold M is convex, and in the regions C_2 and C_3 is concave.

activity of neurons can be realized only in the case of asymmetric connections. Note that the sequential neural activity was also observed in ensembles with inhibitory asymmetric connections [19–21].

Further, Figs. 4-10 show phase portraits and alternating realizations of several possible behaviors of a neural ensemble depending on the external stimulus determined by the values a , b and c . We will assume that the i -th neuron is active if the value of ρ_i exceeds the value of 0.5. Initially, all neurons are inactive. The image point is in the equilibrium state O_1 . In order to activate the neuron, you need to send such an external stimulus to transfer the initial phase point from the equilibrium state O_1 to a small neighborhood of an unstable or saddle heteroclinic cycle G or to a small neighborhood of an invariant manifold M in the case of a saddle heteroclinic cycle G . Depending on the external stimulus, the following dynamics can be obtained:

- excitation of a single neuron (Fig. 4)
- sequential excitation of two neurons (Fig. 5)
- sequential one-time excitation of all three neurons (Figs. 6, 7 and 10)
- sequential multiple excitation of all three neurons (Fig. 8)
- phase trajectory goes to infinity (Fig. 9)

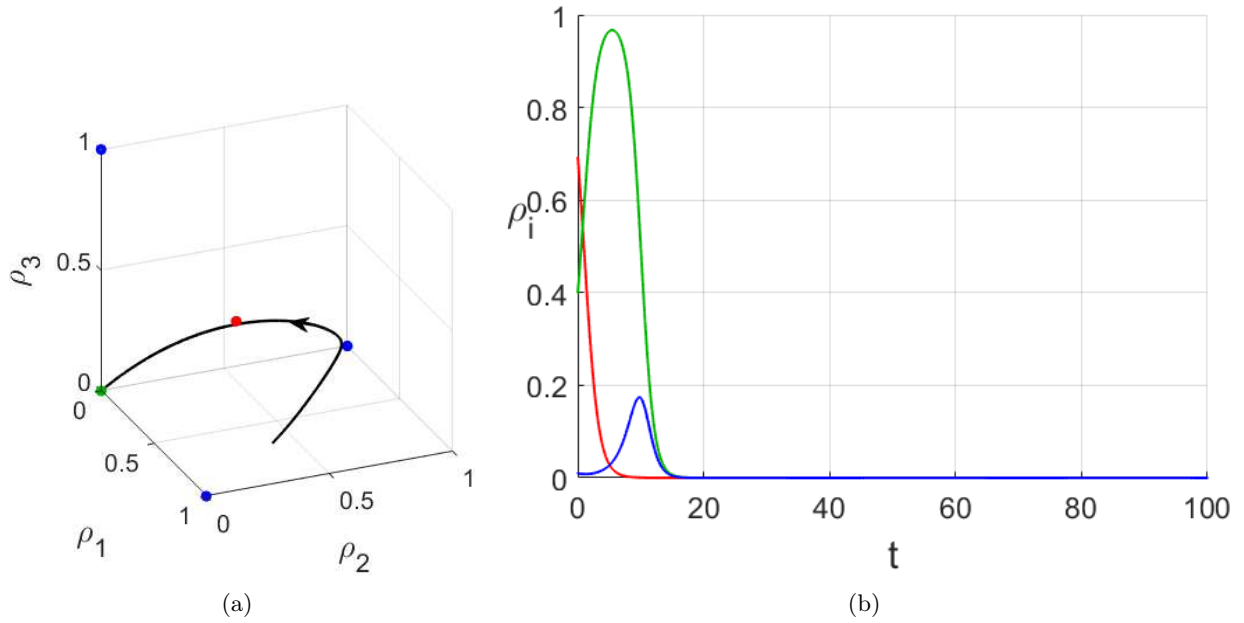


Figure 4: The process of activation and damping. a , b , c parameters are selected so that only one element is activated - the second one. (a) Phase portrait. (b) Time diagram. Here and further, the red curve corresponds to $\rho_1(t)$, the green curve is $\rho_2(t)$, the blue curve is $\rho_3(t)$. Parameter values: $\alpha = 0.1$, $\beta = 1.5$, $a = 0.6917$, $b = 0.4$, $c = 0.01$.

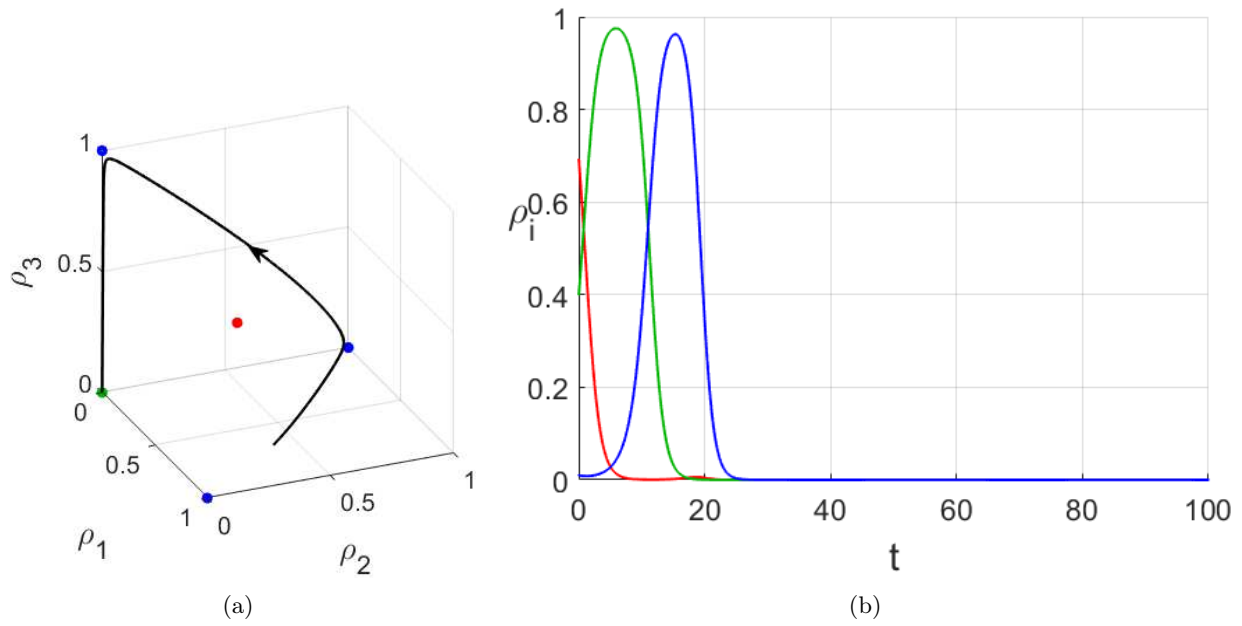


Figure 5: Activation, sequential activity and damping. a, b, c parameters are selected so that only two elements are activated: the second and the third ones. (a) Phase portrait. (b) Time diagram. Parameter values: $\alpha = 0.1, \beta = 1.5, a = 0.69173179, b = 0.4, c = 0.01$.

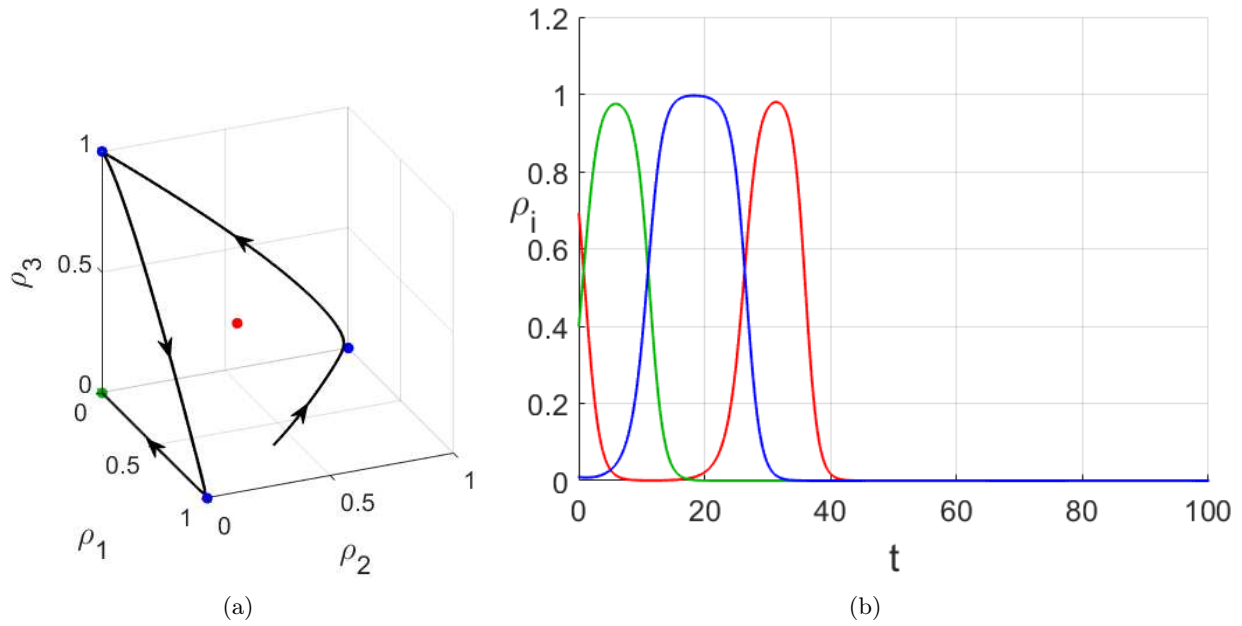


Figure 6: Activation, sequential activity and damping. All three neurons are activated sequentially once. (a) Phase portrait: the phase trajectory takes place in a vicinity of the heteroclinic cycle due to the selection of an external stimuli. (b) Time diagram. Parameter values: $\alpha = 0.1, \beta = 1.5, a = 0.691731794346462, b = 0.4, c = 0.01$.

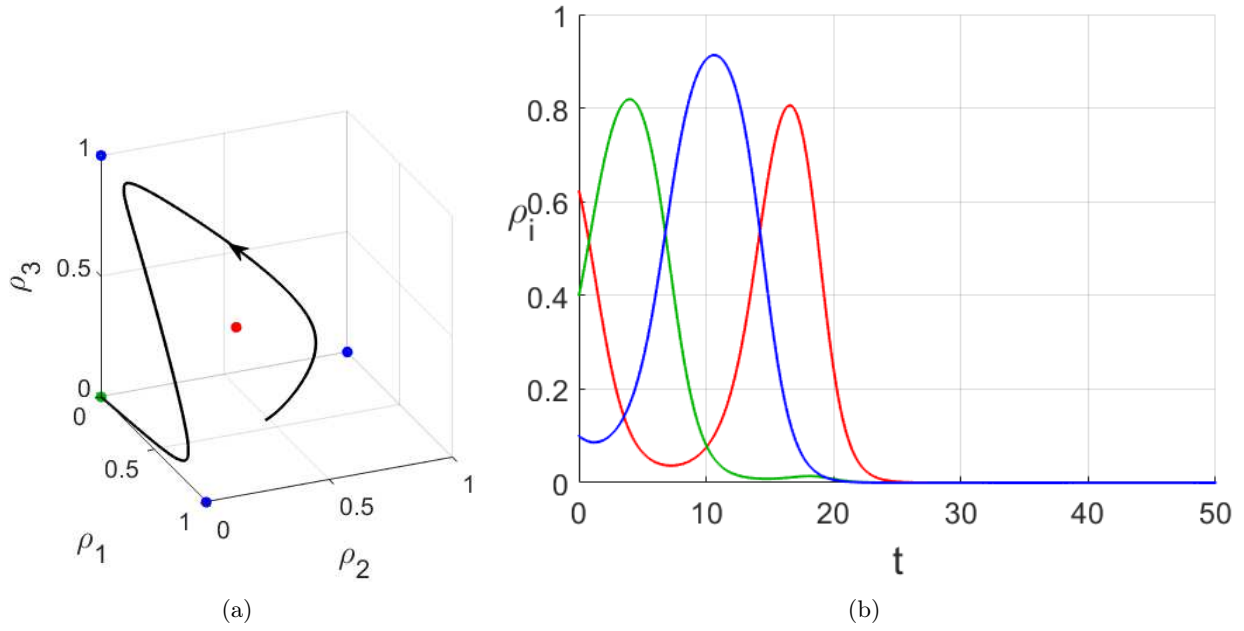


Figure 7: Activation, sequential activity and damping. All three neurons are activated sequentially once. (a) Phase portrait: the phase trajectory does not take place in a vicinity of the heteroclinic cycle due to the selection of an external stimuli. (b) Time diagram. Parameter values: $\alpha = 0.1$, $\beta = 1.5$, $\alpha + \beta < 2$, $a = 0.62313692$, $b = 0.4$, $c = 0.1$.

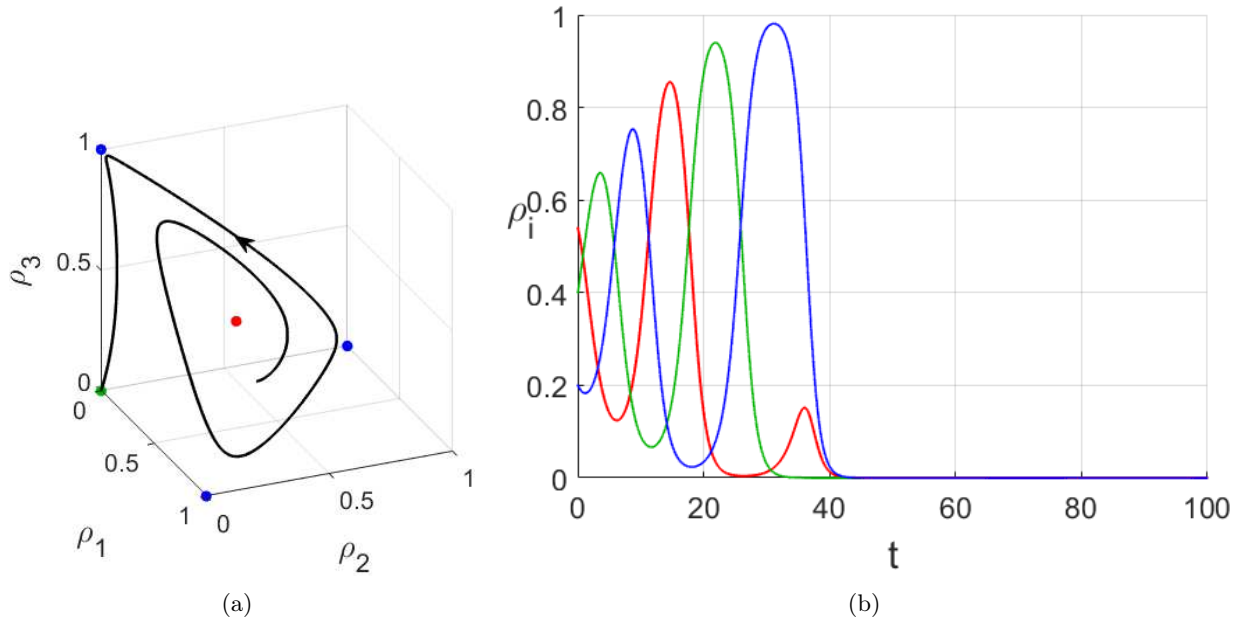


Figure 8: Activation, sequential activity and damping. The second and third neurons are activated twice. The first neuron is activated once. (a) Phase portrait: the phase trajectory takes place in a vicinity of the heteroclinic cycle due to the selection of an external stimuli moving the starting point to the integral manifold M . (b) Time diagram. Parameter values: $\alpha = 0.1$, $\beta = 1.5$, $a = 0.540537789125142$, $b = 0.4$, $c = 0.2$.

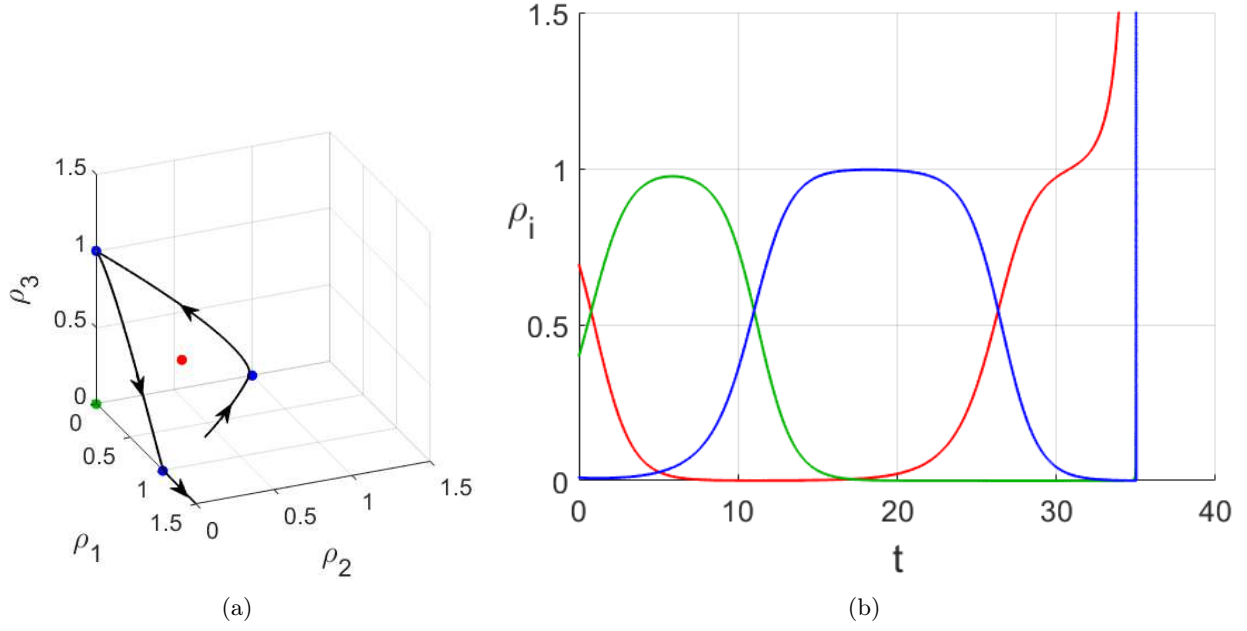


Figure 9: Sequential activity. The phase trajectory goes to infinity. (a) Phase portrait. (b) Time diagram. Parameter values: $\alpha = 0.1$, $\beta = 1.5$, $a = 0.691731794346463$, $b = 0.4$, $c = 0.01$.

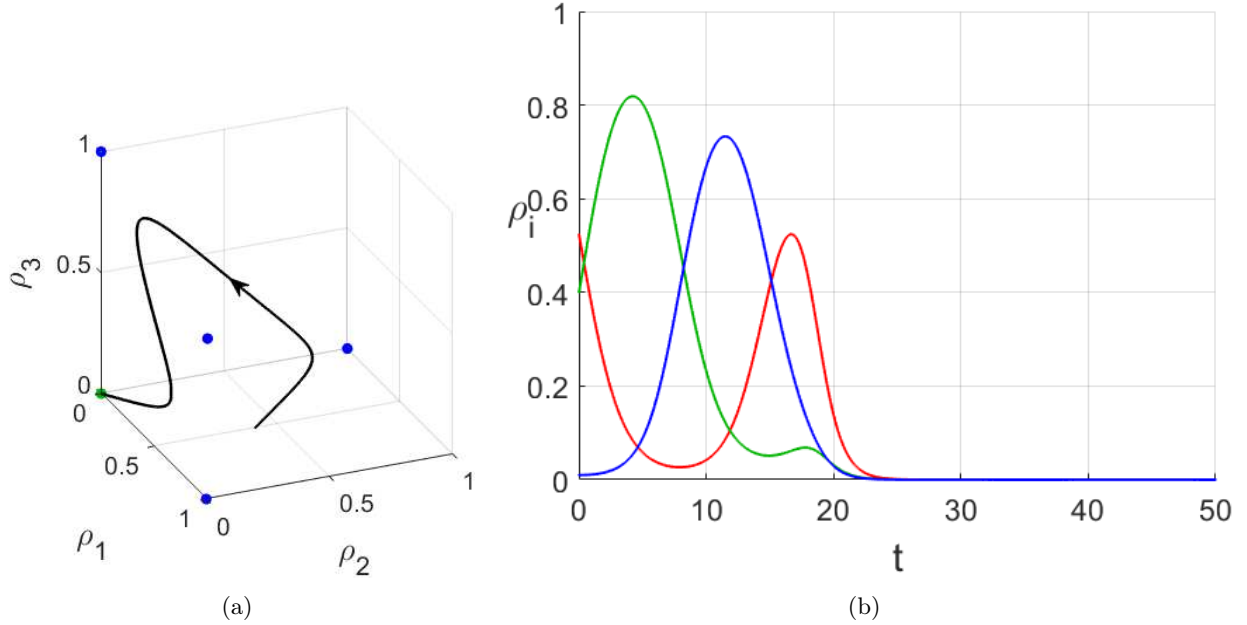


Figure 10: Activation, sequential activity and damping. (a) Phase portrait. (b) Time diagram. Parameter values: $\alpha = 0.4$, $\beta = 1.9$, $\alpha + \beta > 2$, $a = 0.52382217$, $b = 0.4$, $c = 0.01$.

3 The second type system

To eliminate the disadvantage of the first system, the possibility of trajectories going to infinity, in this section we will analyze the dynamics of the ensemble modeled by the following equation

$$\dot{\rho} = \rho(\gamma - \rho)(\rho - 1). \quad (6)$$

Equilibrium state	Eigenvalues	
$O_1(0, 0)$	$-\gamma$	$-\gamma$
$O_2(1, 0)$	$\gamma(\beta - 1)$	$\gamma - 1$
$O_3(0, 1)$	$\gamma(\alpha - 1)$	$\gamma - 1$
$O_4(1 - \alpha\gamma, \gamma)$	$\gamma(\beta(\alpha\gamma - 1) - \gamma + 1)$	$(1 - \alpha\gamma)(\gamma + \alpha\gamma - 1)$
$O_5(\gamma, 1 - \beta\gamma)$	$\gamma(\alpha(\beta\gamma - 1) - \gamma + 1)$	$(1 - \beta\gamma)(\gamma + \beta\gamma - 1)$
$O_6(\gamma, 0)$	$\gamma(\beta\gamma - 1)$	$\gamma(1 - \gamma)$
$O_7(0, \gamma)$	$\gamma(\alpha\gamma - 1)$	$\gamma(1 - \gamma)$
$O_8(\gamma, \gamma)$	$\gamma(1 - \gamma - \alpha\gamma)$	$\gamma(1 - \gamma - \beta\gamma)$
$O_9(\frac{\alpha-1}{\alpha\beta-1}, \frac{\beta-1}{\alpha\beta-1})$	λ_1	λ_2

Table 3: The equilibrium states of Eqs. (8) and their eigenvalues.

The γ parameter is the threshold value of the ensemble's activity. It's value satisfies the inequalities $0 < \gamma < 1$.

Eqs. (6) has three equilibrium states: $\rho = 0$ and $\rho = 1$ are stable and $\rho = \gamma$ is unstable. If the initial condition is $\rho_0 < \gamma$, then the activity of the ρ ensemble decreases and tends to zero. If $\rho_0 > \gamma$, then the activity of the ρ ensemble increases and tends to one. It follows from the above that the set $0 \leq \rho \leq 1$ is invariant.

The model of an ensemble of three connected elements modeled by Eq. (6) has the form

$$\begin{cases} \dot{\rho}_1 = \rho_1(\gamma - \rho_1)(\rho_1 - 1 + \alpha\rho_2 + \beta\rho_3) + a\delta(\rho_1) \\ \dot{\rho}_2 = \rho_2(\gamma - \rho_2)(\rho_2 - 1 + \alpha\rho_3 + \beta\rho_1) + b\delta(\rho_2) \\ \dot{\rho}_3 = \rho_3(\gamma - \rho_3)(\rho_3 - 1 + \alpha\rho_1 + \beta\rho_2) + c\delta(\rho_3) \end{cases} . \quad (7)$$

3.1 Study of a two-dimensional system on an invariant plane $\rho_3 = 0$

Since when one of the conditions $\rho_i = 0$ is met, the i -th equation of Eqs. (7) turns into an identity, then the three planes $\rho_i = 0$ are invariant.

On the invariant plane $\rho_3 = 0$, Eqs. (7) takes the form

$$\begin{cases} \dot{\rho}_1 = \rho_1(\gamma - \rho_1)(\rho_1 - 1 + \alpha\rho_2) + a\delta(\rho_1) \\ \dot{\rho}_2 = \rho_2(\gamma - \rho_2)(\rho_2 - 1 + \beta\rho_1) + b\delta(\rho_2) \end{cases} . \quad (8)$$

The equilibrium states of Eqs. (8) and their eigenvalues are given in Table 3:

The eigenvalues $\lambda_{1,2}$ of the equilibrium state O_9 are too cumbersome and therefore are not given in the table. They are found from the characteristic equation

$$\lambda^2 + \frac{(\alpha-1)(\alpha+\gamma-\alpha\beta\gamma-1)+(\beta-1)(\beta+\gamma-\alpha\beta\gamma-1)}{(\alpha\beta-1)^2} \lambda - \frac{(\alpha-1)(\alpha+\gamma-\alpha\beta\gamma-1)(\beta-1)(\beta+\gamma-\alpha\beta\gamma-1)}{(\alpha\beta-1)^3} = 0.$$

O_9 undergoes Andronov-Hopf bifurcation under the following conditions.

$$\begin{cases} \alpha\beta\gamma(\alpha + \beta - 2) - \alpha^2 - \beta^2 + (2 - \gamma)(\alpha + \beta) + 2\gamma - 2 = 0 \\ \frac{(\alpha-1)(\beta-1)(\alpha\beta\gamma(\alpha\beta\gamma-\alpha-\beta-2\gamma+2)+(\gamma-1)(\alpha+\beta)+\alpha\beta+\gamma^2-2\gamma+1)}{(1-\alpha\beta)^3} > 0 \end{cases} . \quad (9)$$

β parameter can be expressed from the first equation:

$$\beta = \frac{-\alpha^2\gamma + 2\alpha\gamma + \gamma - 2 \pm (\alpha - 1)\sqrt{\alpha^2\gamma^2 + 2\alpha\gamma(2 - \gamma) + \gamma^2 + 4\gamma - 4}}{2(\alpha\gamma - 1)}.$$

At the intersection of this curve in the direction of decreasing β parameter, a stable limit cycle is born in the phase space, which further increases in size and gets into the heteroclinic contour formed by the saddles O_3 , O_4 and O_7 (Fig. 11).

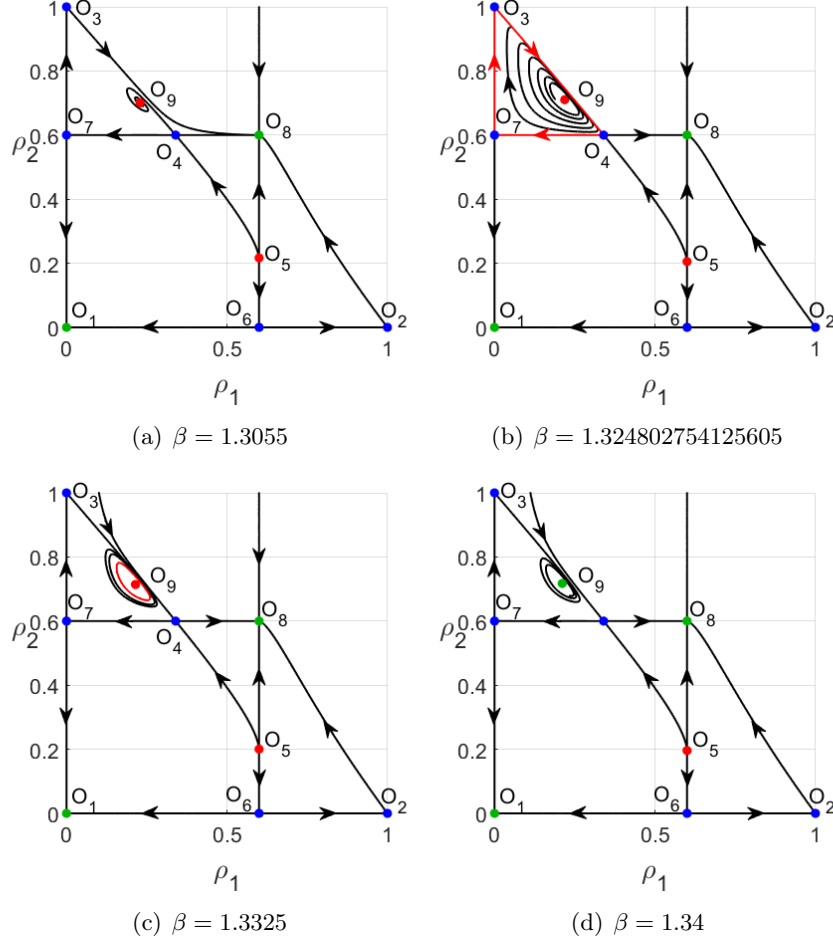


Figure 11: Andronov–Hopf bifurcation and heteroclinic bifurcation. In Figure (b), the heteroclinic cycle connecting the saddles O_3 , O_4 and O_7 is highlighted in red. In Figure (c), a stable limit cycle is highlighted in red. In Figure (d), the limit cycle does not exist, while O_9 is stable. Parameter values: $\alpha = 1.1$, $\gamma = 0.6$.

Similarly with the study of the first type system on invariant planes $\rho_i = 0$, we determine the types of equilibrium states of Eqs. (8) depending on the values of the α and β parameters. The number of regions of the parameter space with different number and type of equilibrium states in this model is greater. It is enough to describe only those regions of the parameter space that lie either above the diagonal $\alpha = \beta$, or intersect it, since in the regions symmetrical with respect to the diagonal, the phase portraits differ only in the numbering of the variables ρ_1 and ρ_2 .

1. O_1 is always a stable node.
2. O_2 is a stable node in the regions A, B, C, H, I ($0 < \beta < 1$) and a saddle in the remaining regions.
3. O_3 is a stable node in the regions $A, B, C, D, E, F, G, H, I, J, K, L$ ($0 < \alpha < 1$) and a saddle in the remaining regions.
4. O_4 is a stable node in the region A and has one negative coordinate in the region S , a saddle in the regions B, C, D, E, F, G, Q, R , and an unstable node in the remaining regions.
5. O_5 is stable node in the regions A, B and has one negative coordinate in the regions F, G, L, N, P, R, S , an unstable node in the region H and a saddle in the remaining regions.

6. O_6 is an unstable node in the regions F, G, L, N, P, R, S ($\beta > \frac{1}{\gamma}$) and a saddle in the remaining regions.
7. O_7 is an unstable node in the region S ($\alpha > \frac{1}{\gamma}$) and a saddle in the remaining regions.
8. O_8 is an unstable node in the regions A and B , a saddle in the regions C, D, E, F and G and a stable node in the remaining regions.
9. O_9 is stable node in the region A , a saddle in the regions B, C, I, Q, R and S , an unstable node in the region H , a stable focus in the regions M and N , an unstable focus in the regions O and P and has one negative coordinate in the remaining regions.

Table 4 provides a summary list of the types of all nine equilibria and the regions in which they exist.

Region	O_1	O_2	O_3	O_4	O_5	O_6	O_7	O_8	O_9
A	SN	SN	SN	SN	SN	S	S	UN	SN
B	SN	SN	SN	S	SN	S	S	UN	S
C	SN	SN	SN	S	S	S	S	S	S
D	SN	S	SN	S	S	S	S	S	-
E	SN	S	SN	S	S	S	S	S	-
F	SN	S	SN	S	-	UN	S	S	-
G	SN	S	SN	S	-	UN	S	S	-
H	SN	SN	SN	UN	UN	S	S	SN	UN
I	SN	SN	SN	UN	S	S	S	SN	S
J	SN	S	SN	UN	S	S	S	SN	-
K	SN	S	SN	UN	S	S	S	SN	-
L	SN	S	SN	UN	-	UN	S	SN	-
M	SN	S	S	UN	S	S	S	SN	SF
N	SN	S	S	UN	-	UN	S	SN	SF
O	SN	S	S	UN	S	S	S	SN	UF
P	SN	S	S	UN	-	UN	S	SN	UF
Q	SN	S	S	S	S	S	S	SN	S
R	SN	S	S	S	-	UN	S	SN	S
S	SN	S	S	-	-	UN	UN	SN	S

Table 4: Types of equilibrium states in all regions of the parameter space (the partitioning into regions is shown in Fig. 12). A dash stands for a presence of a negative coordinate of the equilibrium. SN - stable node, SF - stable focus, UN - unstable node, UF - unstable focus, S - saddle.

In the system under consideration, two bifurcations of equilibrium states are possible: the Andronov-Hopf bifurcation described above and the transcritical bifurcation. Table 5 shows a list of transcritical bifurcations of the equilibrium states of the system.

In Figure 12 the bifurcation diagram of the system described by Eqs. (8) is given for $\gamma = 0.6$.

	O_1	O_2	O_3	O_4	O_5	O_6	O_7	O_8	O_9
$O_1(0, 0)$	-	-	-	-	-	-	-	-	-
$O_2(1, 0)$	-	-	-	-	-	-	-	-	$\beta = 1$
$O_3(0, 1)$	-	-	-	-	-	-	-	-	$\alpha = 1$
$O_4(1 - \alpha\gamma, \gamma)$	-	-	-	-	-	-	$\alpha = \frac{1}{\gamma}$	$\alpha = \frac{1}{\gamma} - 1$	$\beta = \frac{\gamma-1}{\alpha\gamma-1}$
$O_5(\gamma, 1 - \beta\gamma)$	-	-	-	-	-	$\beta = \frac{1}{\gamma}$	-	$\beta = \frac{1}{\gamma} - 1$	$\beta = \frac{\alpha+\gamma-1}{\alpha\gamma}$
$O_6(\gamma, 0)$	-	-	-	-	$\beta = \frac{1}{\gamma}$	-	-	-	-
$O_7(0, \gamma)$	-	-	-	$\alpha = \frac{1}{\gamma}$	-	-	-	-	-
$O_8(\gamma, \gamma)$	-	-	-	$\alpha = \frac{1}{\gamma} - 1$	$\beta = \frac{1}{\gamma} - 1$	-	-	-	-
$O_9(\frac{\alpha-1}{\alpha\beta-1}, \frac{\beta-1}{\alpha\beta-1})$	-	$\beta = 1$	$\alpha = 1$	$\beta = \frac{\gamma-1}{\alpha\gamma-1}$	$\beta = \frac{\alpha+\gamma-1}{\alpha\gamma}$	-	-	-	-

Table 5: Lines on which transcritical bifurcations of equilibrium states occur.

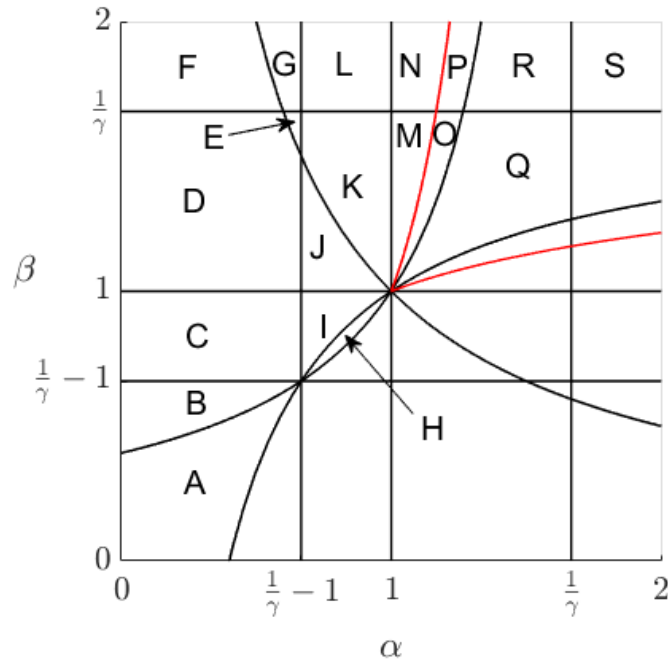


Figure 12: The bifurcation diagram of Eqs. (8) at $\gamma = 0.6$. The black lines correspond to transcritical bifurcations, the red line corresponds to bifurcations of (9).

Phase portraits of Eqs. (7) for all marked areas are shown in Fig. 13. Similarly with the first system, the study of two-dimensional Eqs. (8) should provide information about the dynamics of a three-dimensional system, in which the main attention will be paid again to the existence of a heteroclinic cycle. The trajectories of two-dimensional systems on invariant planes $\rho_i = 0$ will be components of a three-dimensional heteroclinic cycle. As for the first system on invariant planes $\rho_i = 0$, closed trajectories including an unstable node, saddle equilibrium states and a stable node at the origin are of interest. Moreover, the unstable node and one of two saddles should lie on different coordinate axes. Among all other regions on the $\alpha\beta$ -plane F , G and L meet all the requirements. In these regions, there are trajectories connecting unstable nodes, saddle equilibrium states and a stable node O_1 . For example, in Fig. 13 (e), for the regions F and G , there is a contour containing the equilibrium states O_6 , O_8 , O_7 and O_1 . This contour will be an integral part of the heteroclinic cycle in the three-dimensional phase space of the initial system.

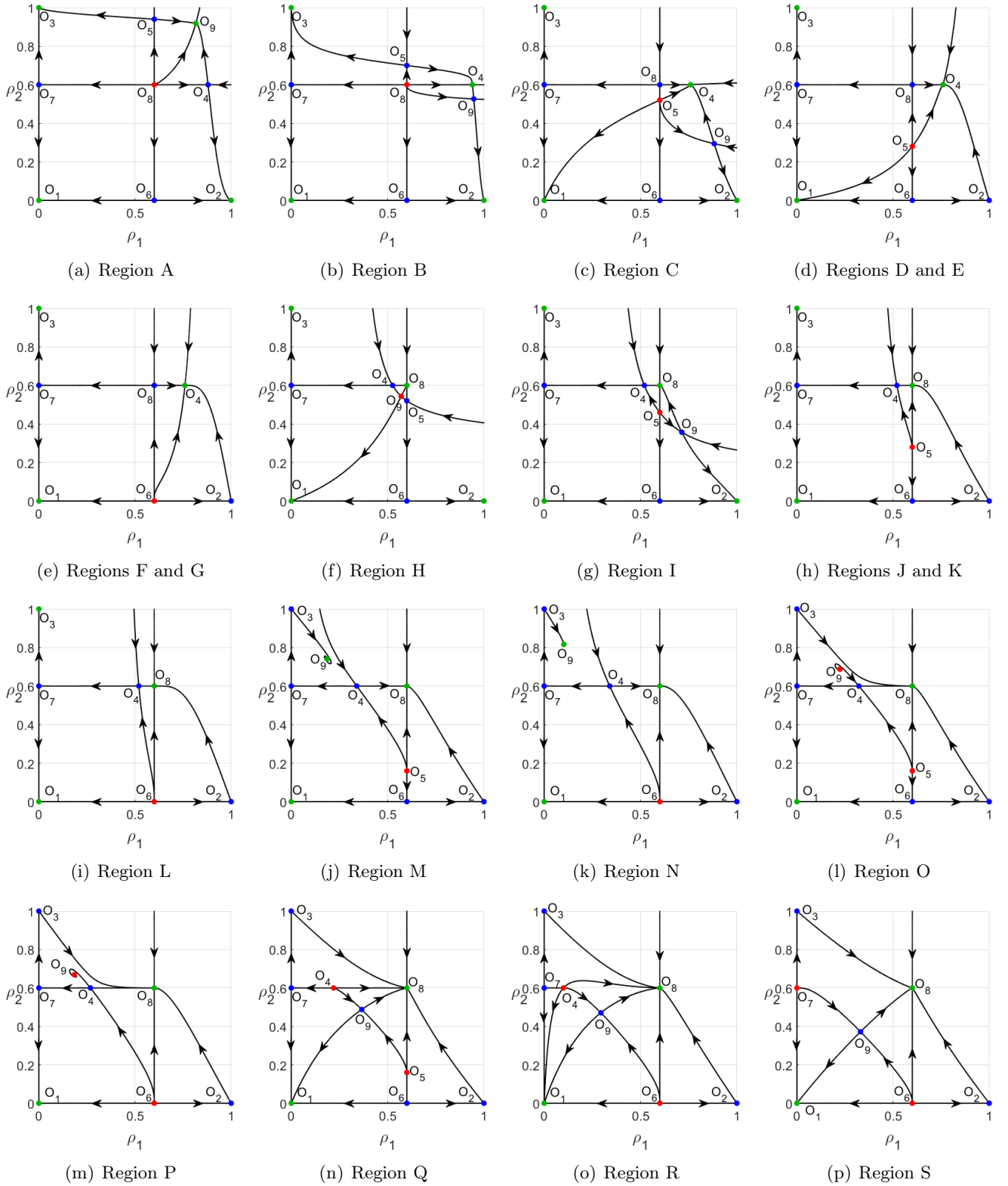


Figure 13: Phase portraits in various regions of Fig. 12.

3.2 A study of Eqs. (7)

The equilibria of Eqs. (7) and their eigenvalues are given in the Table 6.

№	Equilibrium state	Eigenvalues		
1	(0, 0, 0)	$-\gamma$	$-\gamma$	$-\gamma$
2	(1, 0, 0)	$\gamma - 1$	$\gamma(\alpha - 1)$	$\gamma(\beta - 1)$
3	(0, 1, 0)	$\gamma - 1$	$\gamma(\alpha - 1)$	$\gamma(\beta - 1)$
4	(0, 0, 1)	$\gamma - 1$	$\gamma(\alpha - 1)$	$\gamma(\beta - 1)$
5	($\gamma, 0, 0$)	$\gamma(\alpha\gamma - 1)$	$\gamma(\beta\gamma - 1)$	$\gamma(1 - \gamma)$
6	(0, $\gamma, 0$)	$\gamma(\alpha\gamma - 1)$	$\gamma(\beta\gamma - 1)$	$\gamma(1 - \gamma)$
7	(0, 0, γ)	$\gamma(\alpha\gamma - 1)$	$\gamma(\beta\gamma - 1)$	$\gamma(1 - \gamma)$
8	($\gamma, \gamma, 0$)	$\gamma(\alpha\gamma + \beta\gamma - 1)$	$\gamma(1 - \gamma - \alpha\gamma)$	$\gamma(1 - \gamma - \beta\gamma)$
9	($\gamma, 0, \gamma$)	$\gamma(\alpha\gamma + \beta\gamma - 1)$	$\gamma(1 - \gamma - \alpha\gamma)$	$\gamma(1 - \gamma - \beta\gamma)$
10	(0, γ, γ)	$\gamma(\alpha\gamma + \beta\gamma - 1)$	$\gamma(1 - \gamma - \alpha\gamma)$	$\gamma(1 - \gamma - \beta\gamma)$
11	(γ, γ, γ)	$\gamma(1 - \gamma - \alpha\gamma - \beta\gamma)$	$\gamma(1 - \gamma - \alpha\gamma - \beta\gamma)$	$\gamma(1 - \gamma - \alpha\gamma - \beta\gamma)$
12	($1 - \alpha\gamma, \gamma, 0$)	$\gamma(\alpha + \beta\gamma - \alpha^2\gamma - 1)$	$\gamma(\alpha\beta\gamma - \beta - \gamma + 1)$	$-(\gamma - \frac{1}{\alpha})(\gamma - \frac{1}{\alpha+1})$
13	($\gamma, 0, 1 - \alpha\gamma$)	$\gamma(\alpha + \beta\gamma - \alpha^2\gamma - 1)$	$\gamma(\alpha\beta\gamma - \beta - \gamma + 1)$	$-(\gamma - \frac{1}{\alpha})(\gamma - \frac{1}{\alpha+1})$
14	(0, $1 - \alpha\gamma, \gamma$)	$\gamma(\alpha + \beta\gamma - \alpha^2\gamma - 1)$	$\gamma(\alpha\beta\gamma - \beta - \gamma + 1)$	$-(\gamma - \frac{1}{\alpha})(\gamma - \frac{1}{\alpha+1})$
15	($\gamma, 1 - \beta\gamma, 0$)	$\gamma(\beta + \alpha\gamma - \beta^2\gamma - 1)$	$\gamma(\alpha\beta\gamma - \alpha - \gamma + 1)$	$-(\gamma - \frac{1}{\beta})(\gamma - \frac{1}{\beta+1})$
16	($1 - \beta\gamma, 0, \gamma$)	$\gamma(\beta + \alpha\gamma - \beta^2\gamma - 1)$	$\gamma(\alpha\beta\gamma - \alpha - \gamma + 1)$	$-(\gamma - \frac{1}{\beta})(\gamma - \frac{1}{\beta+1})$
17	(0, $\gamma, 1 - \beta\gamma$)	$\gamma(\beta + \alpha\gamma - \beta^2\gamma - 1)$	$\gamma(\alpha\beta\gamma - \alpha - \gamma + 1)$	$-(\gamma - \frac{1}{\beta})(\gamma - \frac{1}{\beta+1})$
18	($\frac{\alpha+\beta\gamma-\alpha^2\gamma-1}{\alpha\beta-1}, \frac{\beta+\alpha\gamma-\beta^2\gamma-1}{\alpha\beta-1}, \gamma$)	λ_1	λ_2	λ_3
19	($\frac{\beta+\alpha\gamma-\beta^2\gamma-1}{\alpha\beta-1}, \gamma, \frac{\alpha+\beta\gamma-\alpha^2\gamma-1}{\alpha\beta-1}$)	λ_1	λ_2	λ_3
20	($\gamma, \frac{\alpha+\beta\gamma-\alpha^2\gamma-1}{\alpha\beta-1}, \frac{\beta+\alpha\gamma-\beta^2\gamma-1}{\alpha\beta-1}$)	λ_1	λ_2	λ_3
21	($\frac{\alpha-1}{\alpha\beta-1}, \frac{\beta-1}{\alpha\beta-1}, 0$)	μ_1	μ_2	μ_3
22	($\frac{\beta-1}{\alpha\beta-1}, 0, \frac{\alpha-1}{\alpha\beta-1}$)	μ_1	μ_2	μ_3
23	(0, $\frac{\alpha-1}{\alpha\beta-1}, \frac{\beta-1}{\alpha\beta-1}$)	μ_1	μ_2	μ_3
24	($1 - \gamma(\alpha + \beta), \gamma, \gamma$)	ν_1	ν_2	ν_3
25	($\gamma, 1 - \gamma(\alpha + \beta), \gamma$)	ν_1	ν_2	ν_3
26	($\gamma, \gamma, 1 - \gamma(\alpha + \beta)$)	ν_1	ν_2	ν_3
27	($\frac{1}{\alpha+\beta+1}, \frac{1}{\alpha+\beta+1}, \frac{1}{\alpha+\beta+1}$)	$\frac{\gamma(1+\alpha+\beta)-1}{\alpha+\beta+1}$	$\frac{(\gamma(1+\alpha+\beta)-1)(\alpha+\beta-2+(\beta-\alpha)\sqrt{3}i)}{2(\alpha+\beta+1)^2}$	$\frac{(\gamma(1+\alpha+\beta)-1)(\alpha+\beta-2-(\beta-\alpha)\sqrt{3}i)}{2(\alpha+\beta+1)^2}$

Table 6: Equilibria of Eqs. (7).

Expressions for the eigenvalues $\lambda_{1,2,3}$, as well as the characteristic equation from which they are determined, are too cumbersome. The eigenvalues $\mu_{1,2,3}$ are determined from the characteristic equation

$$\left(\mu^2 + \frac{(\alpha-1)(\alpha+\gamma-\alpha\beta\gamma-1)+(\beta-1)(\beta+\gamma-\alpha\beta\gamma-1)}{(\alpha\beta-1)^2}\mu - \frac{(\alpha-1)(\alpha+\gamma-\alpha\beta\gamma-1)(\beta-1)(\beta+\gamma-\alpha\beta\gamma-1)}{(\alpha\beta-1)^3}\right)\left(\mu - \frac{\alpha^2+\beta^2+\alpha\beta+\alpha+\beta-1}{\alpha\beta-1}\right) = 0.$$

The eigenvalues $\nu_{1,2,3}$ are determined from the characteristic equation

$$(\nu + (\alpha\gamma + \beta\gamma - 1)(\alpha\gamma + \beta\gamma + \gamma - 1))(\nu^2 - \gamma(\alpha\gamma + \beta\gamma + \gamma - 1)(\alpha + \beta - 2)\nu + \gamma^2(\alpha\gamma + \beta\gamma + \gamma - 1)^2(\alpha - 1)(\beta - 1)) = 0.$$

The subset $0 \leq \rho_1, \rho_2, \rho_3 \leq \gamma$ of the phase space of Eqs. (7) is invariant. In order to simplify the study of the system, we impose conditions on α, β parameters under which the equilibria $O_{12}-O_{26}$ are not in this subset.

$O_{12}-O_{14}$ equilibria have a coordinate $1 - \alpha\gamma$ that goes beyond at $\alpha > \frac{1}{\gamma}$ (region S) and at $\alpha < \frac{1}{\gamma} - 1$ (regions A-L).

$O_{15}-O_{17}$ equilibria have a coordinate $1 - \beta\gamma$ that goes beyond at $\beta > \frac{1}{\gamma}$ (regions F, G, L, N, P, R and S) and at $\beta < \frac{1}{\gamma} - 1$ (regions A and B).

O_{18} - O_{20} equilibria have a coordinate $\frac{\alpha+\beta\gamma-\alpha^2\gamma-1}{\alpha\beta-1}$ that goes beyond in the regions E , F , G , J - N , P and R .

O_{21} - O_{23} equilibria have a coordinates $\frac{\alpha-1}{\alpha\beta-1}$ and $\frac{\beta-1}{\alpha\beta-1}$ that go beyond in the regions A - G and I - P .

O_{24} - O_{26} equilibria have a coordinate $1 - \gamma(\alpha + \beta)$ that goes beyond at $\beta > \frac{1}{\gamma} - \alpha$ (regions F , G , J - S) and at $\beta < \frac{1}{\gamma} - \alpha - 1$ that is never met in the current regions.

Equilibrium state	Eigenvalues		
$O_1(0, 0, 0)$	$-\gamma$	$-\gamma$	$-\gamma$
$O_5(\gamma, 0, 0)$	$\gamma(\alpha\gamma - 1)$	$\gamma(\beta\gamma - 1)$	$\gamma(1 - \gamma)$
$O_6(0, \gamma, 0)$	$\gamma(\alpha\gamma - 1)$	$\gamma(\beta\gamma - 1)$	$\gamma(1 - \gamma)$
$O_7(0, 0, \gamma)$	$\gamma(\alpha\gamma - 1)$	$\gamma(\beta\gamma - 1)$	$\gamma(1 - \gamma)$
$O_8(\gamma, \gamma, 0)$	$\gamma(\alpha\gamma + \beta\gamma - 1)$	$\gamma(1 - \gamma - \alpha\gamma)$	$\gamma(1 - \gamma - \beta\gamma)$
$O_9(\gamma, 0, \gamma)$	$\gamma(\alpha\gamma + \beta\gamma - 1)$	$\gamma(1 - \gamma - \alpha\gamma)$	$\gamma(1 - \gamma - \beta\gamma)$
$O_{10}(0, \gamma, \gamma)$	$\gamma(\alpha\gamma + \beta\gamma - 1)$	$\gamma(1 - \gamma - \alpha\gamma)$	$\gamma(1 - \gamma - \beta\gamma)$
$O_{11}(\gamma, \gamma, \gamma)$	$\gamma(1 - \gamma - \alpha\gamma - \beta\gamma)$	$\gamma(1 - \gamma - \alpha\gamma - \beta\gamma)$	$\gamma(1 - \gamma - \alpha\gamma - \beta\gamma)$
$O_{27}(\frac{1}{\alpha+\beta+1}, \frac{1}{\alpha+\beta+1}, \frac{1}{\alpha+\beta+1})$	$\frac{\gamma(1+\alpha+\beta)-1}{\alpha+\beta+1}$	$\frac{(\gamma(1+\alpha+\beta)-1)(\alpha+\beta-2+(\beta-\alpha)\sqrt{3}i)}{2(\alpha+\beta+1)^2}$	$\frac{(\gamma(1+\alpha+\beta)-1)(\alpha+\beta-2-(\beta-\alpha)\sqrt{3}i)}{2(\alpha+\beta+1)^2}$

Table 7: Equilibria of Eqs. (7) located in the invariant set $0 \leq \rho_1, \rho_2, \rho_3 \leq 1$.

Table 7 contains a list of equilibria and the corresponding eigenvalues located in the invariant set $0 \leq \rho_1, \rho_2, \rho_3 \leq 1$. It is these equilibrium states that will be considered in the study of switching activity associated with the presence of heteroclinic cycles G . Unstable heteroclinic cycles will contain equilibria located on the planes $\rho_i = 0$. The attractors are the equilibrium states O_1 – all neurons are deactivated and O_{27} – all neurons are active. Depending on the amplitude of the external stimuli, the neural ensemble, which was initially in an unexcited state, will resume its initial state or all the neurons of the ensemble will become active. Transients to one state or another depend on the amplitude of the external stimuli. The boundary of the regions of attraction of stable equilibrium states O_1 and O_{11} is an invariant manifold M containing equilibrium states O_5 , O_8 , O_6 , O_{10} , O_7 , O_9 and O_{27} . This manifold intersects ρ_i planes along the trajectories belonging to the heteroclinic cycle G . Switching sequential neural activity is most pronounced in cases when an external stimuli throws the starting point into a small neighborhood of the manifold M . It should be noted that heteroclinic cycles include six (and not three as for the first system) saddle states of equilibrium.

3.2.1 Sequential activity

Three-dimensional system described by Eqs. (7), like Eqs. (2), can exhibit damping sequential activity. Figures. 14 and 15 show examples of such activity. Depending on the external stimuli, the following dynamics can be obtained:

- sequential one-time excitation of all three neurons (Fig. 14 with the subsequent transition of all neurons into an inactive state defined by the equilibrium state O_1 ((a) and (b)) or into the active state determined by the equilibrium state O_{11} ((c) and (d)).
- sequential multiple excitation of all three neurons (Fig. 15 with subsequent damping ((a) and (b)) or with the transition to the active state of all neurons ((c) and (d)).

In addition, as for the first system, activation of one or two neurons is possible.

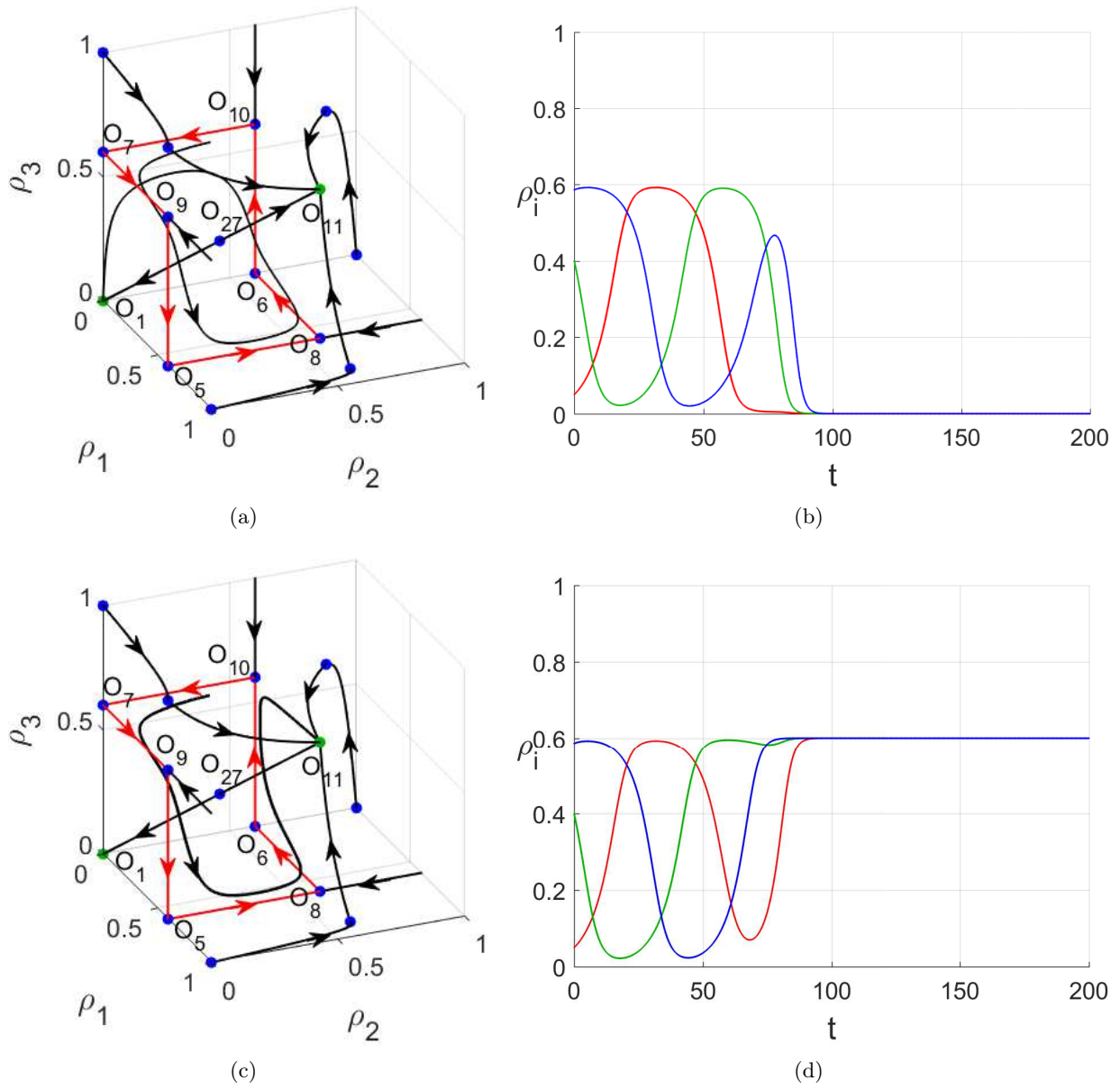


Figure 14: Sequential neural activity. The heteroclinic cycle is marked in red (in Figures (a) and (b)) here and further. Depending on the amplitude of the external stimuli, after each of the elements is activated sequentially once, either deactivation occurs (Figure (a) and (b)), or activation of all elements (Figure (c) and (d)). Parameter values: $\alpha = 0.2$, $\beta = 1.9$, $\gamma = 0.6$. (a), (b) $a = 0.05$, $b = 0.4$, $c = 0.5857$. (c), (d) $a = 0.05$, $b = 0.4$, $c = 0.5858$.

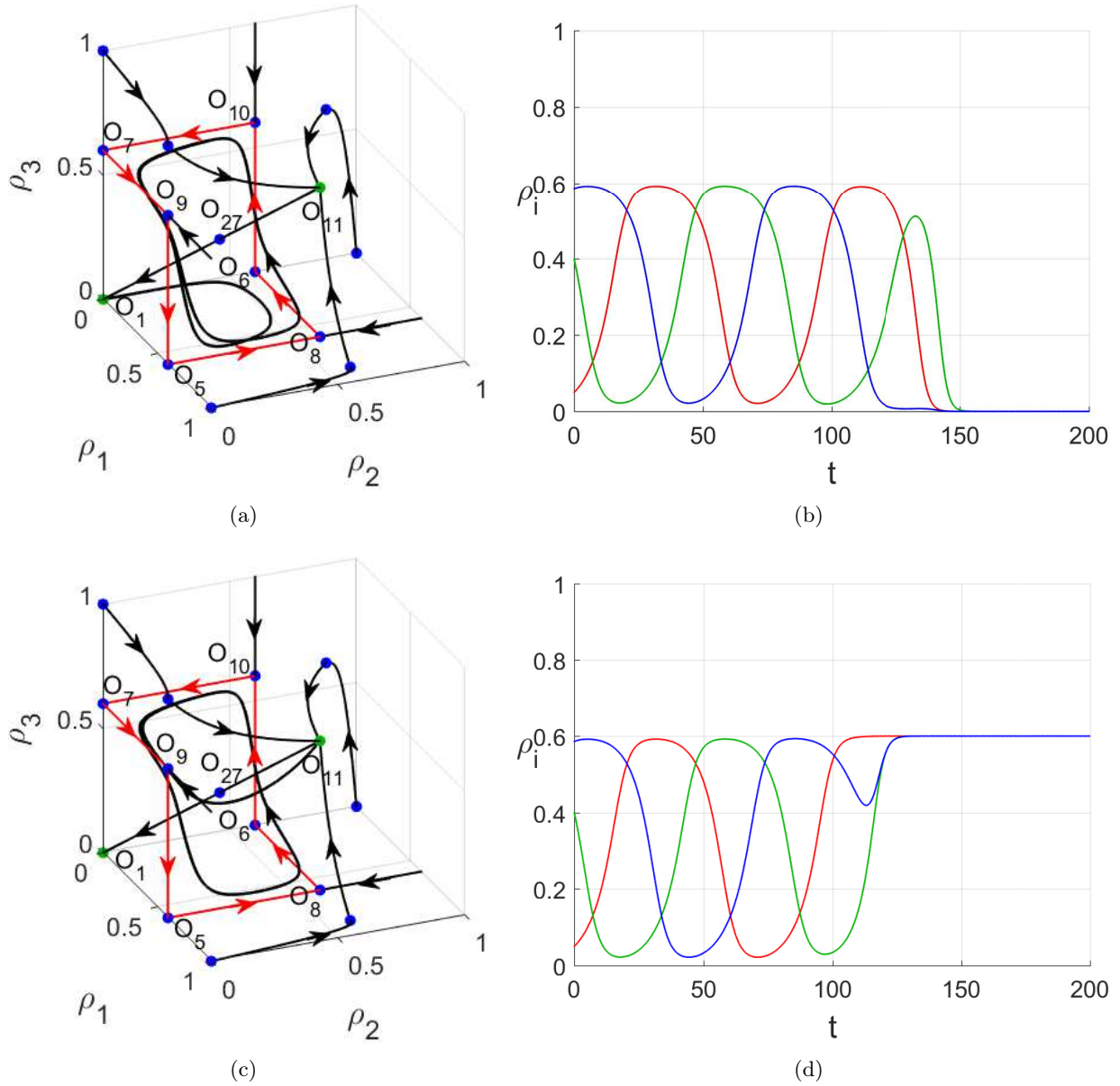


Figure 15: Sequential neural activity. Depending on the amplitude of the external stimuli, after each of the elements is activated sequentially twice, either deactivation occurs (Figure (a) and (b)), or activation of all elements (Figure (c) and (d)). Parameter values: $\alpha = 0.2$, $\beta = 1.9$, $\gamma = 0.6$. (a), (b) $a = 0.05$, $b = 0.4$, $c = 0.585745$. (c), (d) $a = 0.05$, $b = 0.4$, $c = 0.585746$.

4 Summary and conclusions

In this paper

- Two dynamical systems based on the generalized Lotka-Volterra were proposed. Ensembles consist of excitable elements with excitatory couplings.
- The existence of heteroclinic cycles in the phase space of models is shown. The presence of a heteroclinic cycle in the phase space makes it possible to simulate the effect of winnerless competition between modes – sequential switching of ensemble activity between individual neurons or groups of neurons.

- In the proposed models, heteroclinic cycles are not stable, which leads to a complete damping of the ensemble's activity after some time.
- Depending on the external stimuli, one, two or three neurons can be activated.
- The second model, depending on the amplitude of the external stimuli, can demonstrate a damping sequential neural activity with an exit to an inactive state, or to a permanent active state.

The proposed models will be used to construct networks of neural elements and to study their dynamics.

This paper is devoted to Prof. V. N. Belykh, who is outstanding scientist in the field of nonlinear dynamics.

Appendix. Relationship of systems (2) and (7) with the population dynamics equation

When intraspecific competition is taken into account, the dynamics of population size can be described by the following equation [22]

$$\dot{x} = x \left(\frac{b_0 x}{N + x} - d_0 - e x \right), \quad (1)$$

where x is the population size, $b_0 x$ is the specific rate of reproduction (fertility), d_0 is the specific rate of death of individuals (mortality), e is the coefficient characterizing the influence of competition on fertility and mortality, N is the population density at which the average time between consecutive contacts of one the individual is equal to the minimum time between successive fertilizations of the female.

If we decompose the right side of Eq. (1) into a power series, we get

$$\dot{x} = x \left(-d_0 + \left(\frac{b_0}{N} - e \right) x - \frac{b_0 x^2}{N^2} + \frac{b_0 x^3}{N^3} - \frac{b_0 x^4}{N^4} + \frac{b_0 x^5}{N^5} - \dots \right), \quad (2)$$

where the coefficient $\frac{b_0}{N} - e > 0$.

If in Eq. (2) we restrict ourselves to terms of the second order, then we get the equation

$$\dot{x} = x \left(-d_0 + \left(\frac{b_0}{N} - e \right) x \right) = d_0 x \left(-1 + \frac{b_0 - eN}{d_0 N} x \right). \quad (3)$$

By the substitution $\frac{b_0 - eN}{d_0 N} x = \rho$, we get

$$\frac{d\rho}{dt} = d_0 \rho (-1 + \rho). \quad (4)$$

If we now substitute the variable t with $\frac{t}{d_0}$, then we get Eq. (1).

If the equation (2) takes into account terms up to and including the third order, then we get the equation

$$\dot{x} = x \left(-d_0 + \left(\frac{b_0}{N} - e \right) x - \frac{b_0 x^2}{N^2} \right). \quad (5)$$

On condition $\frac{b_0}{N} - e > \frac{2}{N} \sqrt{b_0 d_0}$ polynomial $f(x) = -d_0 + \left(\frac{b_0}{N} - e \right) x - \frac{b_0 x^2}{N^2}$ has two different real roots:

$$x_{1,2} = \frac{\frac{b_0}{N} - e \pm \sqrt{D}}{\frac{2b_0}{N^2}},$$

where $D = \left(\frac{b_0}{N} - e \right)^2 - \frac{4b_0 d_0}{N^2}$ is the discriminant of the polynomial $f(x)$. That is $x_1 > x_2 > 0$. Then Eq. (5) can be written as

$$\dot{x} = \frac{b_0}{N^2} x (x_2 - x)(x - x_1) = \frac{b_0}{N^2} x_1^2 x \left(\frac{x_2}{x_1} - \frac{x}{x_1} \right) \left(\frac{x}{x_1} - 1 \right). \quad (6)$$

By the substitution $\frac{x}{x_1} = \rho$, we get

$$x_1 \frac{d\rho}{dt} = \frac{b_0}{N^2} x_1^3 \rho \left(\frac{x_2}{x_1} - \rho \right) (\rho - 1). \quad (7)$$

By the substitution $\frac{x_1^2 b_0}{N^2} t = \tau$, $\frac{x_2}{x_1} = \gamma$ we get Eq. (6).

Funding

The results in Section 2 were supported by the Ministry of Science and Higher Education of Russian Federation (Project No. 0729-2020-0036), the results in Section 3 were supported by RSF grant # 23-12-00180.

References

- [1] Rabinovich, M. I., Varona, P., Selverston, A. I., and Abarbanel, H. D., Dynamical principles in neuroscience, *Reviews of modern physics*, 2006, vol. 78, no. 4, p. 1213.
- [2] Hahnloser, R. H., Kozhevnikov, A. A., and Fee, M. S., An ultra-sparse code underlies the generation of neural sequences in a songbird, *Nature*, 2002, vol. 419, no. 6902, pp. 65–70.
- [3] Galán, R. F., Sachse, S., Galizia, C. G., and Herz, A. V., Odor-driven attractor dynamics in the antennal lobe allow for simple and rapid olfactory pattern classification, *Neural computation*, 2004, vol. 16, no. 5, pp. 999–1012.
- [4] Levi, R., Varona, P., Arshavsky, Y. I., Rabinovich, M. I., and Selverston, A. I., Dual sensory-motor function for a molluskan statocyst network, *Journal of neurophysiology*, 2004, vol. 91, no. 1, pp. 336–345.
- [5] Guckenheimer, J., and Holmes, P., Structurally stable heteroclinic cycles, in *textitMathematical Proceedings of the Cambridge Philosophical Society*, Cambridge University Press, 1988, vol. 103, no. 1, pp. 189–192.
- [6] Stone, E. and Holmes, P., Random perturbations of heteroclinic attractors, *SIAM Journal on Applied Mathematics*, 1990, vol. 50, no. 3, pp. 726–743.
- [7] Postlethwaite, C. M., and Dawes, J. H., Resonance bifurcations from robust homoclinic cycles, *Nonlinearity*, 2010, vol. 23, no. 3, p. 621.
- [8] Driesse, R. and Homburg, A. J., Resonance bifurcation from homoclinic cycles, *Journal of Differential Equations*, 2009, vol. 246, no. 7, pp. 2681–2705.
- [9] Seliger, P., Tsimring, L. S., and Rabinovich, M. I., Dynamics-based sequential memory: winnerless competition of patterns, *Physical Review E*, 2003, vol. 67, no. 1, p. 011905.
- [10] Afraimovich, V. S., Tristan, I., Huerta, R., and Rabinovich, M. I., Winnerless competition principle and prediction of the transient dynamics in a Lotka–Volterra model, *Chaos: An Interdisciplinary Journal of Nonlinear Science*, 2008, vol. 18, no. 4.
- [11] Rabinovich, M. I., Zaks, M. A., and Varona, P., Sequential dynamics of complex networks in mind: Consciousness and creativity, *Physics Reports*, 2020, vol. 883, pp. 1–32.

- [12] Afraimovich, V.S., Rabinovich, M.I., and Varona, P., Heteroclinic contours in neural ensembles and the winnerless competition principle, *International Journal of Bifurcation and Chaos*, 2004, vol. 14, no. 4, pp. 1195–1208.
- [13] Afraimovich, V.S., Zhigulin, V.P., and Rabinovich, M.I., and Varona, P., On the origin of reproducible sequential activity in neural circuits, *Chaos: An Interdisciplinary Journal of Nonlinear Science*, 2004, vol. 14, no. 4, pp. 1123–1129.
- [14] Rabinovich, M.I., Varona, P., Tristan, I., and Afraimovich, V.S., Chunking dynamics: heteroclinics in mind, *Frontiers in computational neuroscience*, 2014, vol. 8, p. 22.
- [15] Latorre, R., Varona, P., and Rabinovich, M.I., Rhythmic control of oscillatory sequential dynamics in heteroclinic motifs, *Neurocomputing*, 2019, vol. 331, pp. 108–120.
- [16] Durstewitz, D. and Deco, G., Computational significance of transient dynamics in cortical networks, *European Journal of Neuroscience*, 2008, vol. 27, no. 1, pp. 217–227.
- [17] Muezzinoglu, M.K., Tristan, I., Huerta, R., Afraimovich, V.S., and Rabinovich, M.I., Transients versus attractors in complex networks, *International Journal of Bifurcation and Chaos*, 2010, vol. 20, no. 06, pp. 1653–1675.
- [18] Brinkman, B.A., Yan, H., Maffei, A., Park, I.M., Fontanini, A., Wang, J., and La Camera, G., Metastable dynamics of neural circuits and networks, *Applied Physics Reviews*, 2022, vol. 9, no. 1.
- [19] Komarov, M.A., Osipov, G.V., and Suykens, J.A.K., Sequentially activated groups in neural networks, *Europhysics Letters*, 2009, vol. 86, no. 6, p. 60006.
- [20] Komarov, M.A., Osipov, G.V., and Zhou, C.S., Heteroclinic contours in oscillatory ensembles, *Physical Review E*, 2013, vol. 87, no. 2, p. 022909.
- [21] Rabinovich, M.I., Afraimovich, V.S., and Varona, P., Heteroclinic binding, *Dynamical Systems*, 2010, vol. 25, no. 3, pp. 433–442.
- [22] Bazykin, A.D., *Nonlinear dynamics of interacting populations*, World Scientific, 1998.